ACS APPLIED MATERIALS & INTERFACES

Letter

www.acsami.org

Ultralong, Small-Diameter TiO_2 Nanotubes Achieved by an Optimized Two-Step Anodization for Efficient Dye-Sensitized Solar Cells

Xiaoyan Wang,[†] Lidong Sun,[‡] Sam Zhang,*[,†] and Xiu Wang[§]

[†]School of Mechanical and Aerospace Engineering and [§]School of Materials Science and Engineering, Nanyang Technological University, 50 Nanyang Avenue, Singapore 639798, Singapore

[‡]School of Materials Science and Engineering, Chongqing University, Chongqing 400044, P. R. China

Supporting Information

ABSTRACT: An optimized two-step anodization is developed to fabricate ultralong, small-diameter TiO_2 nanotubes, that is, with tube length of up to 31 μm and pore diameter of about 35 nm in this work. This overcomes the length limitation of small diameter tubes that usually presents in conventional one-step anodization. The small tubes with lengths of 23 μm yield a conversion efficiency of 5.02% in dye-sensitized solar cells under nonoptimized conditions.

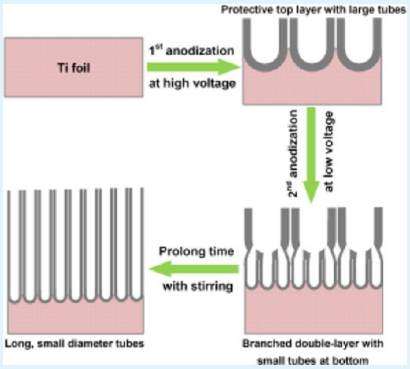

KEYWORDS: *TiO_2, nanotubes, two-step anodization, branched structure, small diameter, dye-sensitized solar cells*

1. INTRODUCTION

Nowadays, nanostructured materials have received substantial research interest because of their extensive applications.[1−3] In particular, TiO_2 nanostructures are among the most important ones, which have been widely used in environmental,[4] biomedical,[5] photocatalytic,[3] and photovoltaic applications.[6] As a promising candidate for low-cost photovoltaics, conventional dye-sensitized solar cells (DSSCs) adopt a thin layer of TiO_2 nanoparticles as photoanodes which provide a large surface area for dye adsorption, leading to efficient light harvesting.[6−9] Considerable research interest has been dedicated toward enhancing cell efficiency. DSSCs based on TiO_2 nanoparticles yielded an efficiency of 7.12% in 1991,[6] 11.1% in 2005,[10] and up to 12.3% in 2011.[11] For further efficiency enhancement, highly ordered TiO_2 nanotube arrays prepared by electrochemical anodization have been developed as an intriguing photoanode, because of their vertical tube alignment for one-dimensional electron transport.[12,13] However, DSSCs based on nanotubes exhibit lower conversion efficiency than that based on nanoparticles, as summarized in one recent review paper.[14] One of the major limiting factors is the relatively lower surface area for dye attachment, as a result of large tube diameter (usually around 100 nm). Consequently, $TiCl_4$ treatment,[15−17] hydrothermal treatment,[18−20] and dipping-rinsing-hydrolysis process[21] have been employed to decorate nanoparticles on tube walls to increase available surface area. Deceasing tube diameter is another promising way to enlarge surface area for higher dye loading.[22−24] It is estimated that when tube diameter is as small as ∼30 nm, nanotubes can provide comparable surface area as conventional nanoparticles of ∼18 nm under the same photoanode volume.[14]

In general, nanotubes of small diameter can be achieved at a low voltage, since tube diameter usually decreases with applied voltage.[25−27] Nevertheless, only tubes of limited length are obtainable under this scenario, because of the low tube growth rate at tube bottoms while high chemical dissolution rate at tube tops.[27] For instance, Zhu et al. prepared nanotubes with pore diameter of 30 ± 4 nm at 20 V, while the tube length was only 5.7 μm after 70 h;[13] Grimes' group fabricated small nanotubes at 20 V, in which the inner tube diameter was ∼45 nm and tube length was 5 μm after 17 h;[28] Schmuki's group produced much smaller tubes of ∼15 nm at 10 V, with the tube length being barely 1 μm after 24 h.[23] Recently, Liu et al. reported that long tubes of 16 μm were produced at 20 V, however the relevant tube diameter was not small enough (i.e., 65 and 75 nm for inner and outer diameter, respectively) as compared to the expected one of ∼30 nm.[29] The large tube length was attributed to an enhanced tube growth rate at elevated temperature (i.e., 50 °C). Such an approach was

Received: November 6, 2013
Accepted: January 21, 2014
Published: January 21, 2014

employed in our previous work to grow nanotubes of similar configuration for use in DSSCs.[17,30] In addition, the tube length was also far from the optimal value of 20−30 μm.[24,31] As such, it is still a challenge to grow such long tubes of small diameter (i.e., ∼30 nm in diameter and ∼30 μm in length).

In our previous work, two-step anodization was proposed to grow long tubes at low voltage (i.e., 15 V). The longest tubes obtained was ∼12 μm at 15 V underneath a protective top layer after 20 h in the presence of stirring.[32] Nevertheless, the presence of an interface hinders the growth of bottom tubes by slowing down mass transport. It is expected that much longer tubes can be obtained in a branched structure under a more protective top layer. In this work, the two-step anodization was optimized further, thus 31-μm-long nanotubes with pore diameter of ∼35 nm were achieved. To the best of our knowledge, such long nanotubes of small diameter have never been reported till date, as compared in Table S1 in the Supporting Information.

2. EXPERIMENTAL SECTION

Electrochemical anodization was performed with a two-electrode configuration at room temperature (∼20 °C), as detailed in our previous work.[19,32,33] The scheme of an optimized two-step anodization is illustrated in Figure 1. In

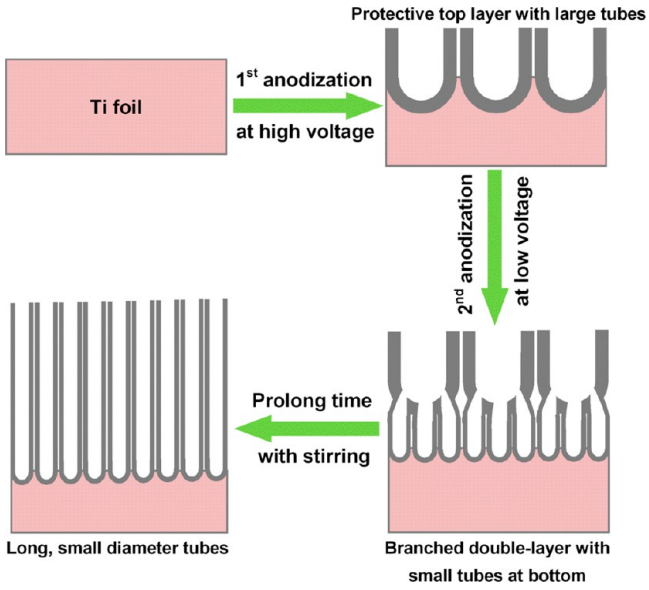

Figure 1. Procedures to fabricate ultralong, small diameter TiO_2 nanotubes by an optimized two-step anodization.

the first anodization, a high voltage of 50 V was adopted to produce a protective top layer, with thick tube walls for a high resistance of chemical dissolution. In this case, a thin top layer was enough to protect the bottom tubes. In the second anodization, the voltage was reduced to 15 V for growth of small nanotubes. The voltage reduction rate was precisely controlled to form branched structure. Magnetic stirring was subsequently applied to further promote tube growth rate at 15 V. After a long enough time, the top layer was dissolved completely, thus exposing the bottom tubes of high aspect ratio. Tube morphologies were characterized by field emission scanning electron microscope (FESEM, JEOL, JSM-7600F). Tube crystal structures were examined by glancing angle X-ray diffraction (GAXRD, PANalytical Empyrean, Cu Kα radiation).

For use in DSSCs, nanotubes were subjected to thermal annealing at 450 °C for 3 h and then assembled into back-illuminated DSSC devices, as described previously.[19] For better cell performance, the nanotubes were also treated in 40 mM $TiCl_4$ aqueous solution at 70 °C for 10 h and then annealed again under the same condition.[17]

3. RESULTS AND DISCUSSION

The first anodization was performed at 50 V for only 15 min to produce a thin protective layer. The applied potential was then decreased to 15 V to grow small tubes. To form the branched structure, voltage reduction rate was an essential factor, as discussed in our recent work.[33] When decreasing voltage from 30 to 15 V, branched structure was obtained with a small reduction rate of 1.5 V/min.[33] However, at a high voltage scheme from 50 to 25 V, tube branching can occur at various voltage reduction rates, as presented in Figure 2a−c. A slow rate of 1 V/min results in tube branching at different levels. A medium rate of 5 V/min or abrupt voltage reduction produces tube branching at the same level. This can be attributed to a high electric field to keep the relatively faster chemical dissolution rate at tube bottoms than that at intertube gaps from 50 to 25 V.[33] Therefore, it takes a shorter time to form branched structure at the high voltage scheme.[34]

Accordingly, in the two-step anodization from 50 to 15 V, the voltage reduction rate was controlled in a stepwise manner, that is, deceasing voltage from 50 to 25 V at 5 V/min and then from 25 to 15 V at 2, 1, or 0.5 V/min. The as-formed double-layered structures are displayed in Figure 2d−f. At 2 V/min, seeding of the second layer occurs at both upper tube bottoms and intertube gaps. A reduction rate of 1 V/min gives rise to tube branching, whereas a few new tubes still grow from intertube gaps. Notably, a much slower rate of 0.5 V/min results in the formation of a desired branched structure, with the bottom tubes penetrating through the upper ones, as highlighted in Figure 2f.

Based on the desired branched structure in Figure 2f, small tubes under the large ones will grow continuously with prolonged anodization time. The top layer grown at 50 V has thick tube walls of ∼27 nm and outer diameters of ∼125 nm (see Figure 2g). The thick walls render a high resistance of chemical dissolution and the large diameters facilitate ion diffusion toward the smaller tubes. The top layer is more than ∼1 μm thick, which is enough to protect the bottom tubes for a long time. To further increase tube growth rate at 15 V, we applied magnetic stirring with a speed of 250 rpm. After 45 h, the top layer is completely dissolved and the bottom tubes reach ∼31 μm with a pore diameter of 35 nm, as depicted in Figure 2h. Such a length is more than four times the reported values (i.e., 5−7 μm) with comparable tube diameter,[13,28,35] resulting in a high aspect ratio of 886, as evidenced in Table S1 in the Supporting Information. In contrast, the conventional one-step anodization at 15 V for 46 h produces nanotubes of only 9.5 μm (see Figure 2i). Therefore, the optimized two-step anodization is effective to grow high-aspect-ratio nanotubes of small diameter.

Through adjusting the top layer thickness and the second anodization duration, length of the small tubes can thus be well-controlled. A thicker top layer can protect the bottom nanotubes for a longer time, hence resulting in longer nanotubes.[32] Nonetheless, too thick a top layer will increase the mass transport distance and therefore slow down the growth rate of the small nanotubes. Consequently, a moderate

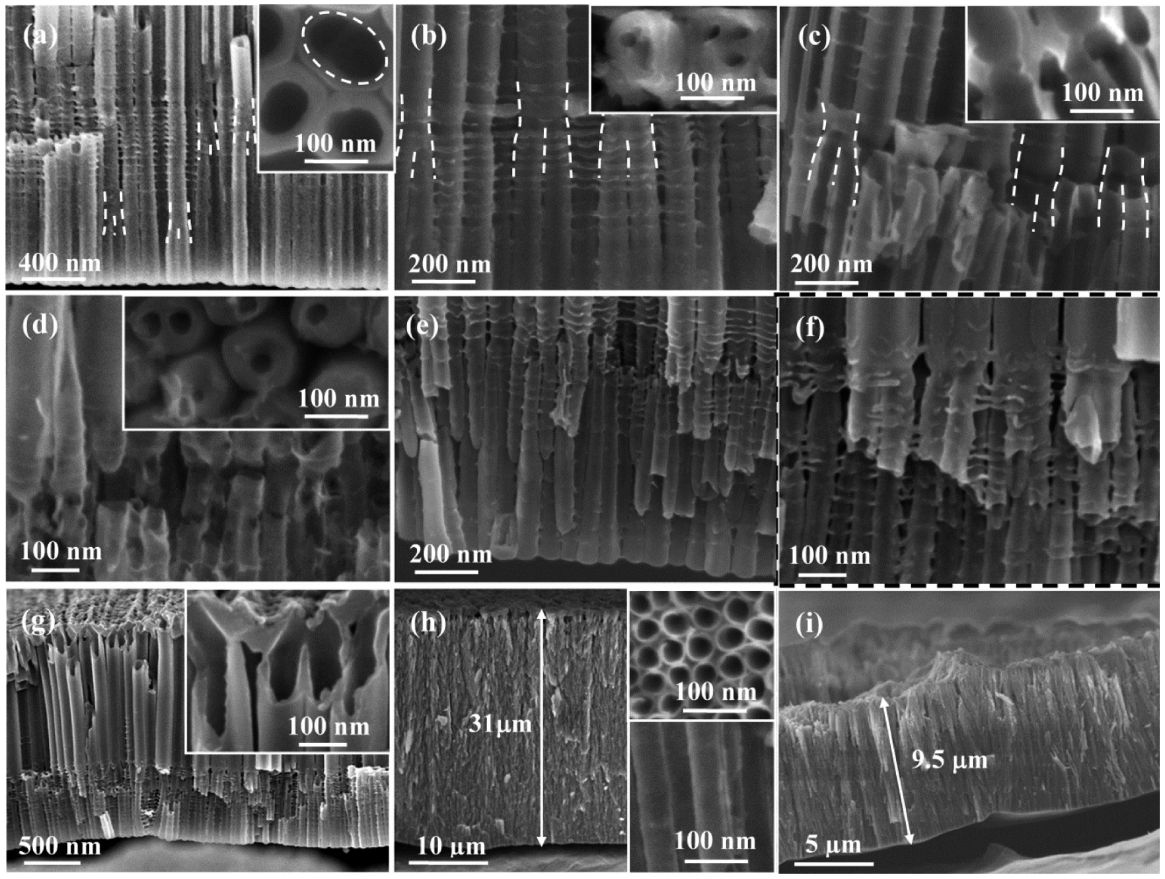

Figure 2. FESEM images of TiO_2 nanotube arrays prepared under different conditions. Top row: two-step anodization from 50 to 25 V at a reduction rate of (a) 1 V/min, (b) 5 V/min, and (c) abrupt reduction. The branching is highlighted by dashed lines and the insets are corresponding top and cross-sectional views of the interfaces. Middle row: two-step anodization from 50 to 15 V by a stepwise reduction rate of 5 V/min from 50 to 25 V and then (d) 2, (e) 1, and (f) 0.5 V/min from 25 to 15 V. (f) is the desired branched structure and highlighted by dashed border. Inset in d is the bottom view of the top layer. Bottom row: (g) double-layered nanotubes grown at 50 V for 15 min and then at 15 V for 1 h with the same voltage reduction rate in f; (h) nanotubes of 31 μm achieved after anodization for 45 h based on the branched structure in g in the presence of stirring; (i) single-layered nanotubes grown by a conventional one-step anodization at 15 V for 46 h. Insets in g and h are corresponding cross-sectional and top views.

thickness of the top layer should be considered for a reasonable growth rate of the small nanotubes.

In DSSC devices, power conversion efficiency increases with tube length and an optimal tube length of ~25 μm is required to produce efficient solar cells.[24,30,36] Accordingly, small nanotubes of ~23 μm were used in this study, with pore diameter of ~35 nm, as presented in Figure 3a. For comparison, 23-μm-long tubes of ~95 nm in diameter were also employed, as shown in Figure 3b. The as-anodized small and large tubes are amorphous, as revealed by GAXRD patterns (see Figure S1 in the Supporting Information). After thermal annealing at 450 °C for 3 h, all the amorphous nanotubes are converted into anatase, which is preferred for application in DSSCs.

Photocurrent−voltage characteristics are presented in Figure 3c. Obviously, with the identical tube length of 23 μm, nanotubes of small diameter yield much higher photocurrent than that of the large ones, i.e., 9.04 vs 5.96 mA/cm^2 for pristine tubes and 12.16 vs 9.13 mA/cm^2 for $TiCl_4$-treated tubes, leaving the other characteristics almost unaffected. For the small tubes, the higher photocurrent results from a larger surface area for dye adsorption, as displayed in Figure 3. This leads to an efficient light harvesting and hence enhanced conversion efficiency. Upon $TiCl_4$ treatment, much higher photovoltage was obtained, consistent with our previous work.[17] This can be ascribed to an improved electron percolation in the treated nanotubes. After $TiCl_4$ treatment, a much higher efficiency of 5.02% was attained for small tubes. Hence, long nanotubes of small diameter are effective to produce highly efficient DSSCs. It is noteworthy that the preliminary study was based on nanotubes without any optimization. A systematic study is required to further promote the cell performance in the future.

4. CONCLUSIONS

Ultralong, small diameter TiO_2 nanotubes are achieved by an optimized two-step anodzation, that is, creating a protective top layer at high voltage, tailoring branched interface by appropriate votage reduction rate and applying stirring to accelerate bottom tube growth. Nanotubes of 31 μm with pore diameter of ~35 nm are thus achieved at 15 V. For an identical length of 23 μm, small tubes of ~35 nm yield an efficiency of 3.48% and 5.02% in DSSCs without and with $TiCl_4$ treatment, respectively, which are much higher than that based on large tubes. This is ascribed to a higher surface area of the small tubes for a larger amount of dye loading. Therefore, long nanotubes of small diameter are favored for highly efficient DSSCs.

dx.doi.org/10.1021/am404966e | ACS Appl. Mater. Interfaces 2014, 6, 1361−1365

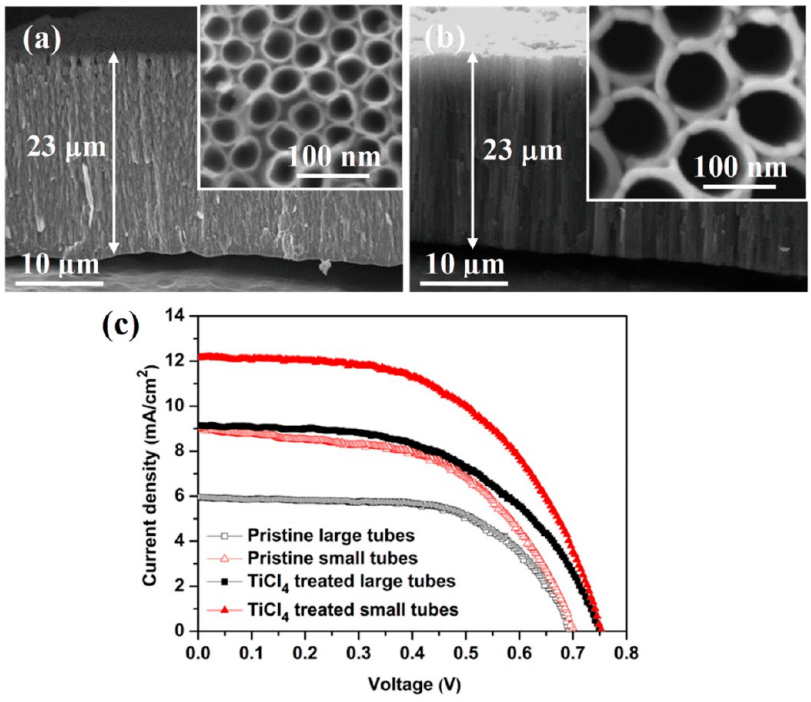

Cell Performance and corresponding amount of dye loading

Samples	J_{sc} (mA/cm^2)	V_{oc} (V)	FF	η (%)	Dye amount (10^{-9}mol/cm^2)
Pristine large tubes	5.96	0.70	0.62	2.59	67.3
Pristine small tubes	9.04	0.70	0.55	3.48	99.9
$TiCl_4$ treated large tubes	9.13	0.75	0.54	3.70	105.6
$TiCl_4$ treated small tubes	12.16	0.75	0.55	5.02	169.2

Figure 3. Morphologies of 23 μm long nanotubes grown with (a) two-step anodization at 50 V for 10 min and then at 15 V for 30 h in the presence of stirring, (b) one-step anodization at 50 V for 4 h. Insets in a and b are corresponding surface morphologies. (c) photocurrent−voltage characteristics of DSSCs based on the pristine and $TiCl_4$-treated small and large tubes. Corresponding cell performance and dye loading amount are computed in the table.

■ ASSOCIATED CONTENT

Supporting Information

Table of diameter and length of TiO_2 nanotubes grown at low voltage; XRD patterns of as-anodized and annealed TiO_2 nanotubes of small and large diameters. This material is available free of charge via the Internet at http://pubs.acs.org.

■ AUTHOR INFORMATION

Corresponding Author

*E-mail: MSYZhang@ntu.edu.sg. Tel: +65-67904400. Fax: +65-67924062.

Notes

The authors declare no competing financial interest.

■ REFERENCES

(1) Ariga, K.; Vinu, A.; Yamauchi, Y.; Ji, Q. M.; Hill, J. P. *Bull. Chem. Soc. Jpn.* **2012**, *85*, 1−32.
(2) Chen, H.; Shao, L.; Li, Q.; Wang, J. *Chem. Soc. Rev.* **2013**, *42*, 2679−2724.
(3) Kubacka, A.; Fernandez-Garcia, M.; Colon, G. *Chem. Rev.* **2012**, *112*, 1555−1614.
(4) Zhang, Q.; Xu, H.; Yan, W. *Nanosci. Nanotechnol. Lett.* **2012**, *4*, 505−519.
(5) Kummer, K. M.; Taylor, E.; Webster, T. J. *Nanosci. Nanotechnol. Lett.* **2012**, *4*, 483−493.
(6) O'Regan, B.; Grätzel, M. *Nature* **1991**, *353*, 737−740.
(7) Grätzel, M. *J. Photochem. Photobiol. C* **2003**, *4*, 145−153.
(8) Grätzel, M. *Inorg. Chem.* **2005**, *44*, 6841−6851.
(9) Grätzel, M. *J. Photochem. Photobiol. A* **2004**, *164*, 3−14.
(10) Nazeeruddin, M. K.; De Angelis, F.; Fantacci, S.; Selloni, A.; Viscardi, G.; Liska, P.; Ito, S.; Takeru, B.; Grätzel, M. *J. Am. Chem. Soc.* **2005**, *127*, 16835−16847.
(11) Yella, A.; Lee, H. W.; Tsao, H. N.; Yi, C. Y.; Chandiran, A. K.; Nazeeruddin, M. K.; Diau, E. W. G.; Yeh, C. Y.; Zakeeruddin, S. M.; Grätzel, M. *Science* **2011**, *334*, 629−634.
(12) Mor, G. K.; Shankar, K.; Paulose, M.; Varghese, O. K.; Grimes, C. A. *Nano Lett.* **2006**, *6*, 215−218.
(13) Zhu, K.; Neale, N. R.; Miedaner, A.; Frank, A. J. *Nano Lett.* **2007**, *7*, 69−74.
(14) Sun, L.; Zhang, S.; Wang, Q.; Zhao, D. *Nanosci. Nanotechnol. Lett.* **2012**, *4*, 471−482.
(15) Roy, P.; Kim, D.; Paramasivam, I.; Schmuki, P. *Electrochem. Commun.* **2009**, *11*, 1001−1004.
(16) Kim, D.; Roy, P.; Lee, K.; Schmuki, P. *Electrochem. Commun.* **2010**, *12*, 574−578.
(17) Sun, L.; Zhang, S.; Wang, X.; Sun, X. W.; Ong, D. Y.; Wang, X.; Zhao, D. *ChemPhysChem* **2011**, *12*, 3634−3641.
(18) Ye, M. D.; Xin, X. K.; Lin, C. J.; Lin, Z. Q. *Nano Lett.* **2011**, *11*, 3214−3220.

(19) Wang, X.; Sun, L.; Zhang, S.; Wang, X.; Huo, K.; Fu, J.; Wang, H.; Zhao, D. *RSC Adv.* **2013**, *3*, 11001−11006.
(20) Pan, X. A.; Chen, C. H.; Zhu, K.; Fan, Z. Y. *Nanotechnology* **2011**, *22*, 1−7.
(21) Lin, L.-Y.; Chen, C.-Y.; Yeh, M.-H.; Tsai, K.-W.; Lee, C.-P.; Vittal, R.; Wu, C.-G.; Ho, K.-C. *J. Power Sources* **2013**, *243*, 535−543.
(22) Ghicov, A.; Albu, S. P.; Hahn, R.; Kim, D.; Stergiopoulos, T.; Kunze, J.; Schiller, C. A.; Falaras, P.; Schmuki, P. *Chem. Asian J.* **2009**, *4*, 520−525.
(23) Liu, N.; Lee, K.; Schmuki, P. *Electrochem. Commun.* **2012**, *15*, 1−4.
(24) Roy, P.; Kim, D.; Lee, K.; Spiecker, E.; Schmuki, P. *Nanoscale* **2010**, *2*, 45−59.
(25) Bauer, S.; Kleber, S.; Schmuki, P. *Electrochem. Commun.* **2006**, *8*, 1321−1325.
(26) Yasuda, K.; Schmuki, P. *Electrochim. Acta* **2007**, *52*, 4053−4061.
(27) Sun, L.; Zhang, S.; Sun, X. W.; He, X. *J. Electroanal. Chem.* **2009**, *637*, 6−12.
(28) Prakasam, H. E.; Shankar, K.; Paulose, M.; Varghese, O. K.; Grimes, C. A. *J. Phys. Chem. C* **2007**, *111*, 7235−7241.
(29) Liu, X.; Lin, J.; Chen, X. *RSC Adv.* **2013**, *3*, 4885−4889.
(30) Sun, L.; Zhang, S.; Wang, X.; Sun, X. W.; Ong, D. Y.; Kyaw, A. K. K. *Energy Environ. Sci.* **2011**, *4*, 2240−2248.
(31) Sun, L.; Zhang, S.; Sun, X.; He, X. *J. Nanosci. Nanotechnol.* **2010**, *10*, 4551−4561.
(32) Wang, X.; Zhang, S.; Sun, L. *Thin Solid Films* **2011**, *519*, 4694−4698.
(33) Wang, X.; Sun, L.; Zhang, S.; Zhao, D. *Electrochim. Acta* **2013**, *107*, 200−208.
(34) Chen, B.; Lu, K. *Langmuir* **2012**, *28*, 2937−2943.
(35) Macak, J. M.; Tsuchiya, H.; Taveira, L.; Aldabergerova, S.; Schmuki, P. *Angew. Chem., Int. Ed.* **2005**, *44*, 7463−7465.
(36) Varghese, O. K.; Paulose, M.; Grimes, C. A. *Nat. Nanotechnol.* **2009**, *4*, 592−597.